



Research papers

Operational protocol for the sighting and tracking of Portuguese man-of-war in the southeastern Bay of Biscay: Observations and modeling

L. Ferrer ^{*}, N. Zaldua-Mendizabal, A. Del Campo, J. Franco, J. Mader, U. Cotano, I. Fraile, A. Rubio, Ad. Uriarte, A. Caballero

AZTI-Marine Research, Herrera Kaia, Portualdea z/g, 20110 Pasaia, Spain



ARTICLE INFO

Article history:

Received 6 February 2014

Received in revised form

19 December 2014

Accepted 23 December 2014

Available online 31 December 2014

Keywords:

Bay of Biscay

Physalia physalis

Portuguese man-of-war

ROMS

SOFT

WRF

ABSTRACT

This paper describes the operational protocol established in the southeastern Bay of Biscay (study area) for the sighting and tracking of Portuguese man-of-war. This action protocol combines sightings of Portuguese man-of-war at sea with hourly surface currents and winds obtained with the Regional Ocean Modeling System (ROMS) and the Weather Research and Forecasting model (WRF), respectively. These data are used in the Sediment, Oil spill and Fish Tracking model (SOFT) to estimate the drift of Portuguese man-of-war. Here we provide information on sightings of Portuguese man-of-war in the study area and show the most relevant results of the SOFT calibration obtained using trajectories from eight satellite pop-up tags for fish tracking. These tags have similar characteristics (such as weight and density) to the Portuguese man-of-war that reach the study area. In 2012 and 2013, there were a total of 48 sightings of Portuguese man-of-war, most of them located in the Zarautz beach area (Basque Country coast). The SOFT calibration shows that the tag drift is mainly controlled by the wind. With winds from the southern and western sectors (third quadrant), SOFT is able to reproduce the tag drift using surface current velocities estimated as ~1.8% of the WRF wind velocities. The SOFT simulations carried out using the ROMS current velocities (with or without the WRF wind velocities) do not improve the results.

© 2015 Elsevier Ltd. All rights reserved.

1. Introduction

One of the most common problems in summer along coasts and beaches is the arrival of gelatinous organisms, which may cause a significant socioeconomic impact (Condon et al., 2013). Identifying the causes of the proliferation of these organisms and predicting their physical behavior in the marine environment by numerical tools are of interest for a correct and appropriate management of the problem, thus responding to the affected sectors of society. The present work describes the operational protocol established in the southeastern Bay of Biscay for the sighting and tracking of *Physalia physalis* (phylum: Cnidaria, class: Hydrozoa, order: Siphonophora, suborder: Cystonectae, family: Physaliidae). The aim of this protocol is to prevent the stings of this gelatinous organism in bathing areas.

Physalia physalis, better known as Portuguese man-of-war or blue bottle, is not a true jellyfish. This species is a colony of numerous polyps (Totton and Mackie, 1960; Bardi and Marques, 2007). One of the polyps develops into a gas-filled float that looks like a sail (pneumatophore) and others develop into digesting

polyps (gastrozooids), reproductive polyps (gonozooids) and long defending and hunting tentacles (dactylozooids). The float is asymmetric and the tentacles are equipped with stinging capsules that serve to paralyze and trap prey. If these tentacles come in contact with human skin, they can inflict significant damage. Fig. 1 shows the organization of the colony in a Portuguese man-of-war.

Nowadays, the response of Portuguese man-of-war and jellyfish to physical forcing (both in terms of life cycle and advective transport) is rather unknown, which makes difficult its implementation in biophysical models. However, some researchers have attempted to describe the physical behavior of these organisms, as for example Iosilevskii and Wehs (2009). These researchers addressed the sailing of Portuguese man-of-war; in particular, the hydrodynamics of their trailing tentacles, and the interaction between these tentacles and the float to obtain the best sailing performance. In their study, the tracked Portuguese man-of-war were observed sailing with their sails aligned with the wind under strong wind conditions.

In addition to describing the operational protocol for the sighting and tracking of Portuguese man-of-war, the main objectives of this work are the following: (1) To provide information on sightings of Portuguese man-of-war in the southeastern Bay of Biscay; and (2) to calibrate the Lagrangian particle-tracking model

* Corresponding author. Fax: +34 946 572 555.

E-mail address: l.ferrer@azti.es (L. Ferrer).

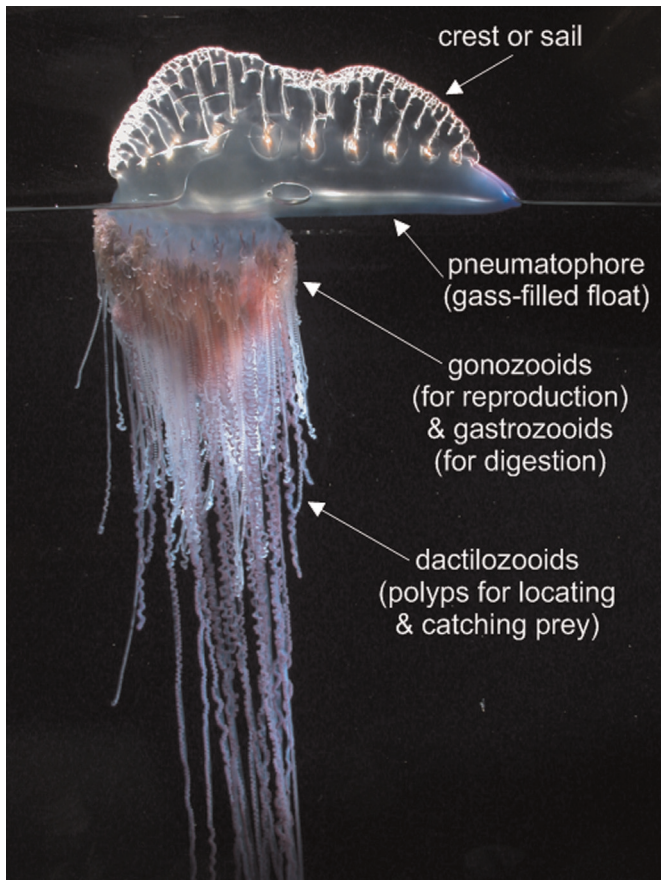


Fig. 1. Organization of the colony in a Portuguese man-of-war (*Physalia physalis*). Photograph by Casey Dunn.

used in the operational protocol to estimate the drift of Portuguese man-of-war. This calibration is important because this model is the base to estimate the risk of Portuguese man-of-war along the Basque Country coast.

2. Methodology

2.1. Study area

The Bay of Biscay extends approximately from 43.5°N to 48.5°N in latitude, and from Cape Ortegal, northwestern Spain (8°W), to the French coast (1°W). The water circulation in the Bay of Biscay is weak ($\sim 1\text{--}2 \text{ cm s}^{-1}$) and is characterized by the frequent presence of eddies together with a persistent poleward flow (see Fig. 2). This poleward flow is also known as the slope current (Pingree and Le Cann, 1992a, 1992b; Koutsikopoulos and Le Cann, 1996; Puillat et al., 2004; Serpette et al., 2006; Ferrer and Caballero, 2011). Over the Basque Country shelf, the circulation in the upper water column is mainly controlled by the wind, tides, and density currents induced by river discharges (Ibáñez, 1979; González et al., 2004; Fontán et al., 2006; Caballero et al., 2008; Ferrer et al., 2009).

Several papers have demonstrated that surface currents in the ocean are significantly dependent on wind and wave conditions (e.g., Ursell, 1950; Longuet-Higgins, 1953, 1960; Hasselmann, 1970; Pollard, 1970; Huang, 1979; Wu, 1983; Jenkins, 1989; Perrie et al., 2003; Tang et al., 2007; and Song, 2009). These authors conclude that the effects of wind and waves on the classical Ekman currents are important, as they change the nature of the Ekman layer. More information about the characteristics of this layer can be found in

Ekman (1905). In the Bay of Biscay and in the northwestern coastal area of Spain, Sotillo et al. (2008) and Abascal et al. (2009, 2012) analyzed buoy trajectories and compared them with simulated trajectories. For their simulations, they used a combination of outputs from numerical models (wind, waves and ocean currents) and HF radar data. The conclusion of these papers is that the estimation of surface currents in the ocean with numerical models should include the effects of wind and waves in the upper centimeters of the water column, in order to reduce the discrepancies between the classical Ekman theory and the observations. These effects can be particularly significant for floating objects such as Portuguese man-of-war.

2.2. Observing system

The operational protocol established in the southeastern Bay of Biscay for the sighting and tracking of Portuguese man-of-war was launched in the summer of 2012. It consists of an observing system and a modeling system (Fig. 3). The observing system involves the participation of several stakeholders: Department of Security of the Basque Government, AZTI, Euskalmet and EKP (meteorological agency and marinas of the Basque Country, respectively), SASEMAR (Spanish maritime safety agency), City Council of Donostia-San Sebastián, Provincial Councils of Gipuzkoa and Bizkaia, and Red Cross. Evidently, the participation of fishermen and any marine user in this observing system is crucial, because most of the information on sightings of Portuguese man-of-war and jellyfish is provided by them.

Prior to the summer season, the first step of the observing system is the delivery of informative leaflets, posters and sighting registration forms in ports, beaches, associations, university and coastal tourist sites. This is carried out by the Department of Security of the Basque Government. In addition, e-mails are sent to the people involved in the early warning system. The informative leaflets consist of: (1) an identification guide of the main species of jellyfish, including the Portuguese man-of-war, listed in order of abundance on the Basque Country coast and indicating their level of hazard; and (2) a brief version of the action protocol established in case of sighting (Ferrer et al., 2013). The informative posters are exclusively dedicated to the Portuguese man-of-war.

If there are sightings of gelatinous organisms, the first step is to identify the species. If this is a Portuguese man-of-war, people are asked to call 112 (SOS-Deiak, Basque emergency service) or contact SASEMAR (via VHF channel 16), indicating the following: GPS or approximate location, time, number of organisms and their approximate dimensions. In this case, SOS-Deiak fills in a data sheet that sends immediately to AZTI in order to run a Lagrangian particle-tracking model and obtain a 96-h forecast of the drift of Portuguese man-of-war. This forecast, with information of possible impacts along the Basque Country coast, is sent to SOS-Deiak, who distributes it among the competent authorities and the people involved in the early warning system. In case of no Portuguese man-of-war, people are asked to fill in a form at www.itsasnet.com. This information is of great value since it allows us to make a database on the different species of gelatinous organisms that have reached the Basque Country coast.

2.3. Modeling system

Regarding the modeling system established for the tracking of Portuguese man-of-war, two models are run by AZTI. The first one is the Regional Ocean Modeling System (ROMS), which is the hydrodynamic model used to estimate current, temperature and salinity fields in the Bay of Biscay. ROMS is an evolution of the S-Coordinate Rutgers University Model (SCRUM), as described by Song and Haidvogel (1994). It has been expanded to include a

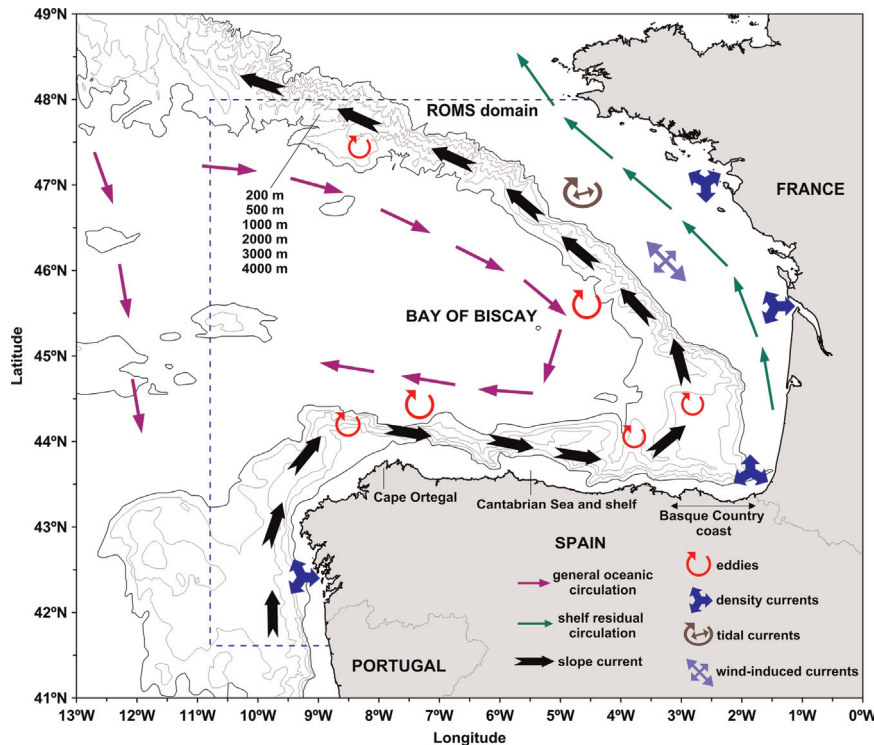


Fig. 2. General ocean circulation in the Bay of Biscay (adapted from Ferrer et al., 2009). The dashed lines indicate the ROMS domain.

variety of features, such as: high-order advection-schemes; accurate pressure gradient algorithms; several subgrid-scale parameterizations; atmospheric, oceanic and benthic boundary layers; biological modules; radiation boundary conditions; and data assimilation.

ROMS has been developed at Rutgers University, but also at the University of California and the Institut de Recherche pour le Développement (IRD). In this work, we used the ROMS_AGRIF version developed at IRD (Debreu et al., 2012). The numerical aspects of ROMS have been described in detail by Shchepetkin and McWilliams (2005). ROMS has been used to model the water circulation in different regions of the world ocean (e.g., Haidvogel et al., 2000; Penven et al., 2001; Marchesiello et al., 2003; Di Lorenzo et al., 2004; and Choi and Wilkin, 2007), including the study area (e.g., Ferrer et al., 2007, 2009; Ferrer and Caballero, 2011; Caballero et al., 2014; and Laiz et al., 2014).

The ROMS domain used in the operational system covers the Bay of Biscay, extending from 42°N to 48°N and from 11°W to 0.5°W, with a 4-km horizontal resolution (Fig. 2). Vertically, the water column is divided into 32 sigma-coordinate levels; these are more concentrated within the surface waters, where most of the variability occurs. In order to obtain a realistic bathymetry for ROMS, an interpolation (following an optimization analysis) of the 2 min digital Elevation TOPOgraphic model (ETOPO2), General Bathymetric Chart of the Oceans (GEBCO) and International Bathymetric Chart of the Mediterranean (IBCM) data sets was carried out. This bathymetry was smoothed to ensure stable and accurate simulations (Haidvogel et al., 2000). With this ROMS configuration, 96-h forecasts are obtained daily. In addition, a hindcast for the period 2008–2012 was carried out for the modeling system calibration.

The atmospheric forcing inputs used in ROMS are provided by MeteoGalicia (meteorological agency of Galicia). These data (with hourly resolution) are obtained using the Weather Research and Forecasting model (WRF). A more detailed description of this model can be found in Skamarock et al. (2005). Two one-way

nested domains are used in WRF (Fig. 4): the parent domain covers part of the North Atlantic Ocean and southwestern Europe, with a 36-km horizontal resolution, while the child domain covers the Iberian Peninsula and the Bay of Biscay, with a 12-km horizontal resolution. The initial and boundary conditions for the WRF parent domain are provided by the National Centers for Environmental Prediction (NCEP). These data (three-hourly and 0.5° horizontal resolution analysis/forecasts) are obtained using the Global Forecast System (GFS). For the WRF child domain, these conditions are obtained from the parent domain results. The WRF variables used in ROMS are the following: wind and air temperature at 10 and 2 m above sea level, respectively; precipitation rate; relative humidity; and long and short wave radiation fluxes. The air-sea heat and momentum fluxes are calculated using the bulk formulae of Fairall et al. (1996, 2003).

In ROMS, the conditions applied to the open boundaries are a combination of outward advection and radiation, together with a flow-adaptive nudging term for relaxation toward prescribed external conditions (Marchesiello et al., 2001). In the operational system, these external conditions are estimated using the World Ocean Atlas 2009, WOA09 (Antonov et al., 2010; Locarnini et al., 2010). This atlas consists of a description of data analysis procedures and horizontal maps of annual, seasonal and monthly climatological distribution fields of several commonly-measured ocean variables. This information is obtained at selected standard depth levels of the world ocean on a 1° latitude-longitude grid. In the 2008–2012 hindcast, the conditions applied to the open boundaries were obtained from the Estimating the Circulation and Climate of the Ocean (ECCO) project. This project, which combines general circulation modeling with observations, is funded by the National Oceanographic Partnership Program (NOPP). From this project, we used the 10-d and 1° horizontal resolution product.

For the tidal forcing, data from the OSU TOPEX/Poseidon Global Inverse Solution (TPXO) are used. This is a global model of ocean tides, developed at Oregon State University, which best-fits (in a least-squares sense) the Laplace Tidal Equations and along-track

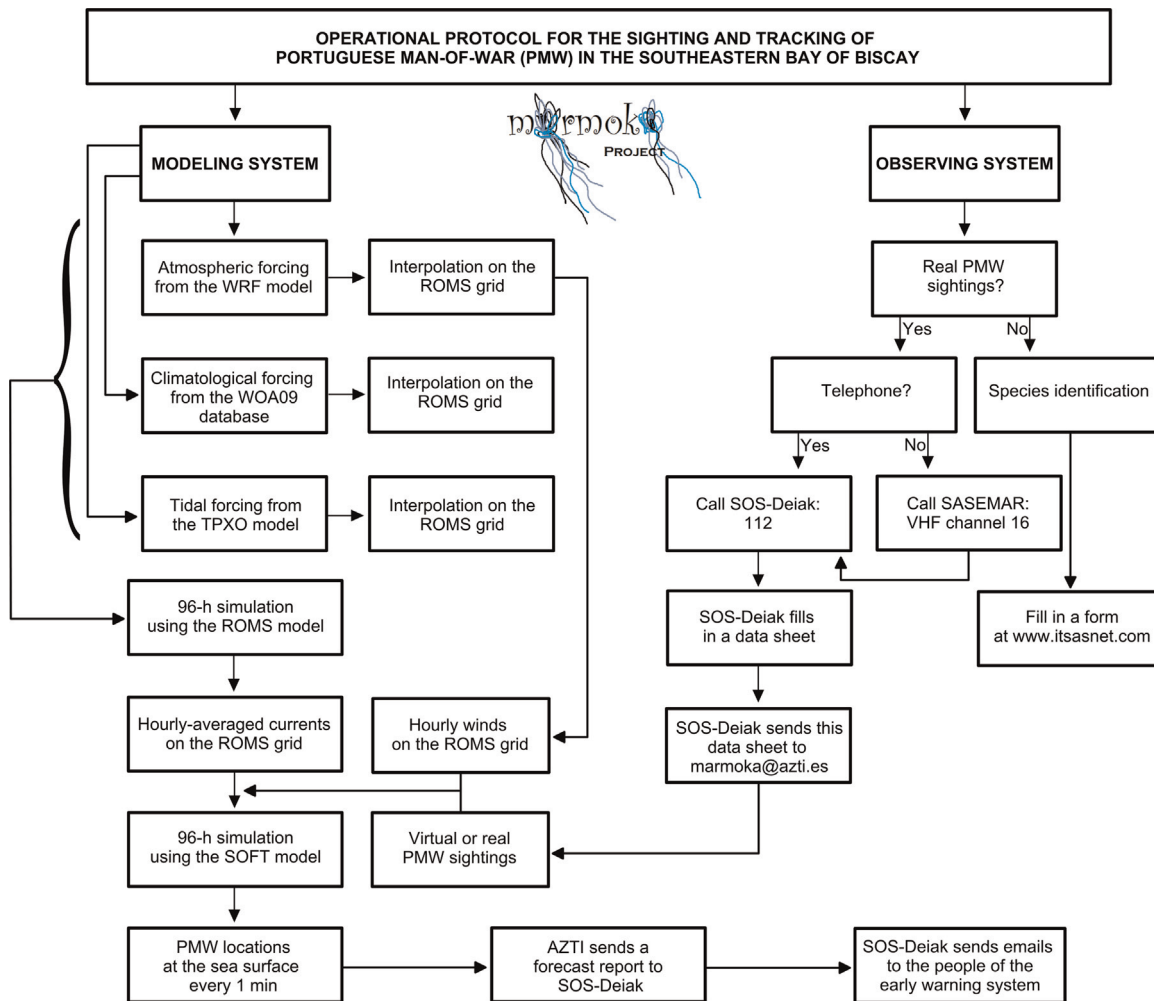


Fig. 3. Operational protocol for the sighting and tracking of Portuguese man-of-war in the southeastern Bay of Biscay.

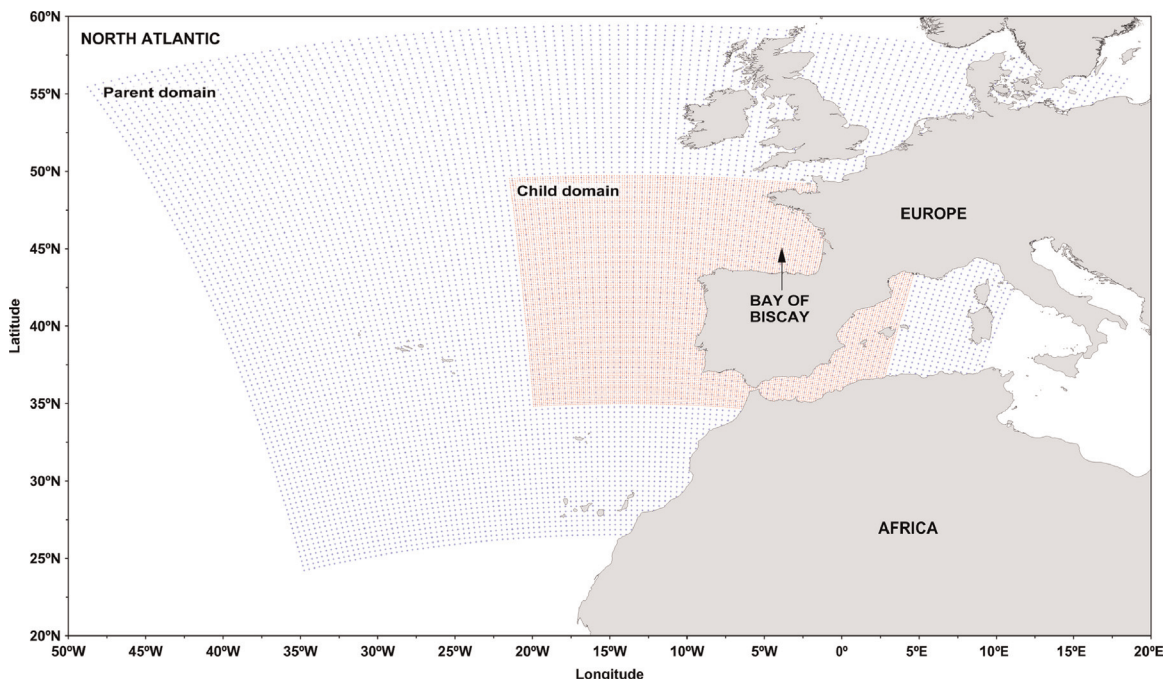


Fig. 4. Sea grid points of the WRF parent and child domains.

averaged data from the TOPEX/Poseidon orbit cycles (Egbert et al., 1994). The tides are provided as complex amplitudes of Earth-relative sea-surface elevation for eight primary (M_2 , S_2 , N_2 , K_2 , K_1 , O_1 , P_1 and Q_1), two long period (M_f and M_m) and three non-linear (M_4 , MS_4 and MN_4) harmonic constituents, on a 1440×721 , $1/4^\circ$ resolution full global grid. These harmonics are introduced into ROMS through the open boundaries, using the Flather condition (Marchesiello et al., 2001).

The winds and currents obtained with WRF and ROMS, respectively, are used as inputs for the Sediment, Oil spill and Fish Tracking model (SOFT). This is a Lagrangian particle-tracking model, developed by Ferrer et al. (2004), which is used in the operational protocol to simulate the drift of Portuguese man-of-war. The total surface current velocity, U , used in SOFT to estimate this drift is a combination of the ROMS current velocity, U_{ROMS} , and the WRF wind velocity, U_{WRF} . This can be expressed as:

$$U = C_{ROMS} U_{ROMS} + C_{WRF} U_{WRF}$$

where C_{ROMS} and C_{WRF} are calibration coefficients for the ROMS and WRF model outputs, respectively. In our case, C_{ROMS} is equal to 0 or 1, and C_{WRF} , the wind drag coefficient, ranges from 0 to 0.04. On the right-hand side of this equation, the second term includes the effects of local wind and sea wave-induced Stokes drift on the drift of floating objects. The Stokes drift is the net displacement of surface water due to the orbital motion and nonlinear dynamics of surface waves. The swell wave-induced Stokes drift is not included in this equation. When $C_{ROMS}=0$ or $C_{WRF}=0$, SOFT uses the outputs obtained with WRF or ROMS, respectively, to estimate the drift of Portuguese man-of-war. If $C_{ROMS}=1$ and $C_{WRF}>0$, SOFT uses the outputs from both models to estimate this drift. SOFT has the option to include random turbulent velocity terms to

parameterize unresolved subgrid-scale phenomena. In this work, this option was deactivated. The method used for the movement of particles is based on the 4th order Runge–Kutta scheme (Benson, 1992).

In the operational system, C_{ROMS} and C_{WRF} are equal to 1 and 0.03, respectively. This C_{WRF} value is commonly applied in the surface drift of oil spills (Fallah and Stark, 1976; Wu, 1983). However, these coefficients must be estimated for each specific floating object. In SOFT, this is done by means of an automatic calibration methodology that provides the optimal C_{WRF} value and decides the C_{ROMS} value (0 or 1). This methodology is based on the minimization of the non-dimensional index s (normalized cumulative Lagrangian separation) proposed by Liu and Weisberg (2011). This index is defined as:

$$s = \sum_{i=1}^N d_i / \sum_{i=1}^N l_{oi}$$

where d_i is the separation distance between the modeled and observed end points of the Lagrangian trajectories at time step i after the initialization, l_{oi} is the associated cumulative length of the observed trajectory, and N is the total number of time steps. Note that the smaller the s value, the better the performance, with $s=0$ implying a perfect fit between observations and simulations. In conventional model skill scores, a higher value means a better model performance. In this sense, Liu and Weisberg (2011) proposed the following trajectory model skill score:

$$ss = \begin{cases} 1 - s/n, & s \leq n \\ 0, & s > n \end{cases}$$

where n is a non-dimensional tolerance threshold. In our case, n is

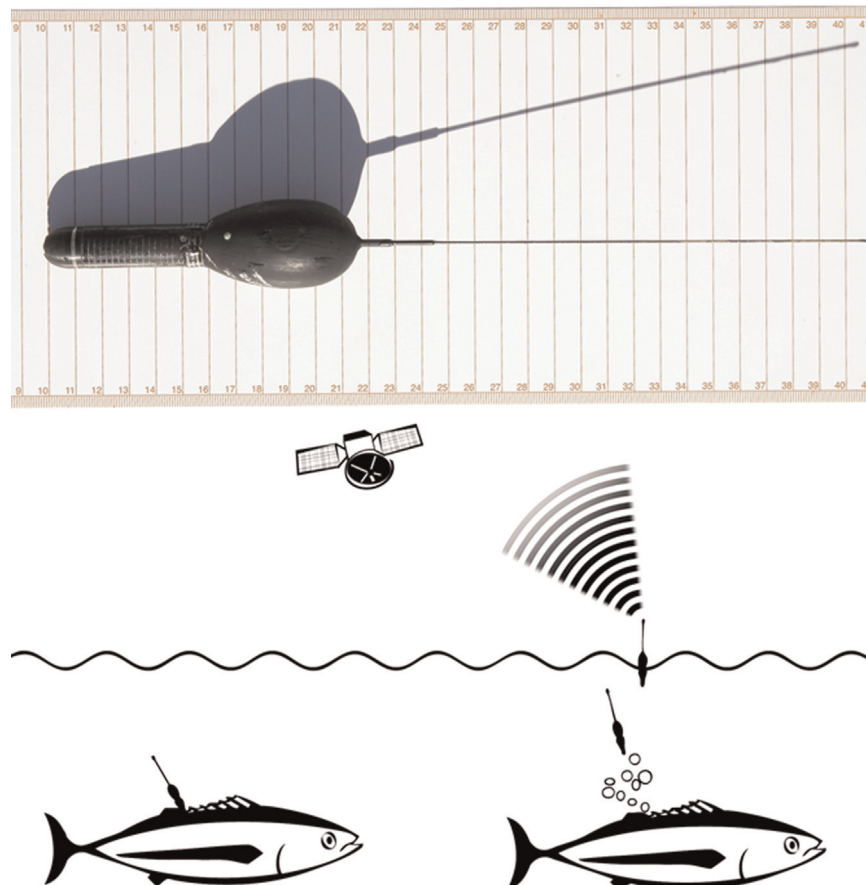


Fig. 5. Satellite pop-up tag for fish tracking. Photograph and drawing by Igaratza Fraile and Eneko Fraile, respectively.

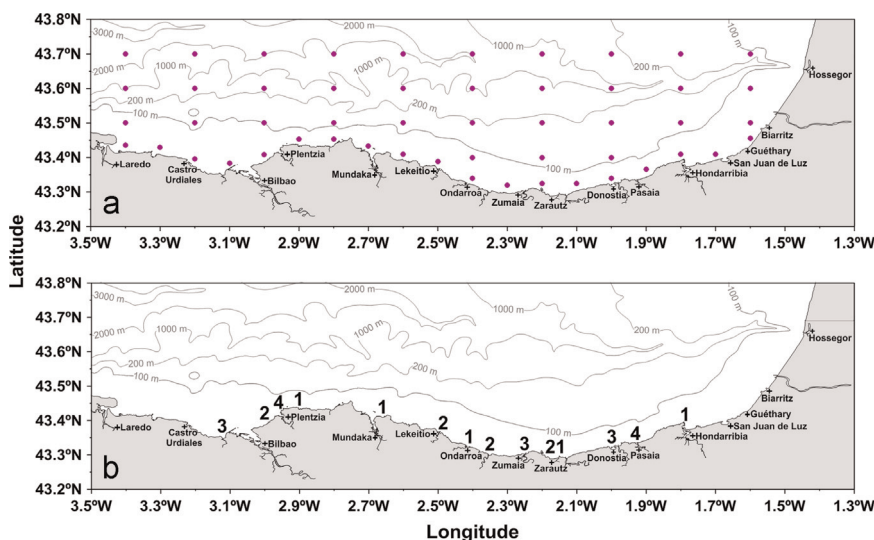


Fig. 6. (a) Initial locations (52 points) of the virtual sightings of Portuguese man-of-war used daily in SOFT; and (b) sightings of Portuguese man-of-war registered in 2012 and 2013 along the Basque Country coast.

Table 1
Sightings of Portuguese man-of-war registered in 2012 and 2013 along the Basque Country coast.

Date (dd/mm/yyyy hh:mm)	Place	Location	Number
20/07/2012 18:45	Zumaia (beach)	43.3°N–2.25°W	3
22/07/2012 16:30	Zarautz (beach)	43.29°N–2.16°W	2
28/07/2012 19:00	Getaria (Malkorbe beach)	43.3°N–2.2°W	1
31/07/2012 16:00	Zarautz (offshore)	43.3°N–2.17°W	2
01/08/2012 19:21	Zarautz (habor)	43.29°N–2.18°W	1
07/08/2012 19:55	Zarautz (habor)	43.29°N–2.18°W	1
08/08/2012 16:15	Armintza (habor)	43.43°N–2.9°W	1
09/08/2012 13:23	Orio (offshore)	43.31°N–2.13°W	5
11/08/2012 12:15	Saturrarán (beach)	43.32°N–2.41°W	1
11/08/2012 12:32	Zarautz (beach)	43.29°N–2.16°W	1
11/08/2012 12:58	Donostia (Ondarreta beach)	43.32°N–2.0°W	1
11/08/2012 15:38	La Arena (beach)	43.35°N–3.12°W	2
11/08/2012 16:57	Deba (Santiago beach)	43.3°N–2.35°W	1
12/08/2012 18:30	Zarautz (beach)	43.29°N–2.16°W	2
15/08/2012 08:00	Donostia (offshore)	43.33°N–2.01°W	1
17/08/2012 18:29	Plentzia (offshore)	43.42°N–2.95°W	1
18/08/2012 21:20	Plentzia (offshore)	43.42°N–2.95°W	1
19/08/2012 15:19	Pasai (habor)	43.33°N–1.93°W	4
20/08/2012 17:17	La Arena (beach)	43.35°N–3.12°W	1
21/08/2012 16:00	Zarautz (beach)	43.29°N–2.16°W	1
21/08/2012 19:46	Lekeitio (offshore)	43.36°N–2.48°W	1
22/08/2012 14:13	Lekeitio (Karraspío beach)	43.36°N–2.49°W	1
23/08/2012 14:20	Zarautz (beach)	43.29°N–2.16°W	1
25/08/2012 14:43	Gorliz (beach)	43.41°N–2.94°W	2
31/08/2012 14:00	Getaria (Malkorbe beach)	43.3°N–2.2°W	1
03/09/2012 18:45	Sopela (Arrietara beach)	43.39°N–3°W	1
03/09/2012 18:45	Ibarrangelua (Laga beach)	43.41°N–2.66°W	1
28/05/2013 18:18	Donostia (Zurriola beach)	43.34°N–1.98°W	1
18/06/2013 14:00	Zarautz (beach)	43.29°N–2.16°W	1
09/07/2013 17:17	Deba (Santiago beach)	43.3°N–2.35°W	1
14/07/2013 12:55	Zarautz (beach)	43.29°N–2.16°W	2
16/07/2013 14:58	Hondarribia (offshore)	43.4°N–1.79°W	1
23/08/2013 17:52	Sopela (Arrietara beach)	43.39°N–3°W	1

the maximum s value obtained in the SOFT simulations. This skill score ranges from 0 (no skill) to 1 (perfect simulation). The simulated trajectories with a s value higher than 0.8 are considered acceptable. In our simulations, this value implies a mean separation distance between 2.2 and 9.2 km, depending on the observed trajectory length.

Trajectory data from Portuguese man-of-war shaped drifting buoys would be necessary for the application of the calibration methodology. But at present, there are no data from this type of buoys. These buoys should have similar characteristics (such as

weight and density) to the organisms that reach the Basque Country coast. In 2015, efforts will be made to design them and obtain trajectory data. In this study, the modeling system calibration was carried out with available trajectories from satellite pop-up tags for fish tracking (see Fig. 5). These tags pop free of the tagged fish at a preprogrammed time, float to the sea surface and beam their accumulated data via satellite to scientists to reveal where these fish moved and what ocean temperatures they favored. During the battery lifetime (between a few days and four weeks), these tags are floating at the sea surface and are advected

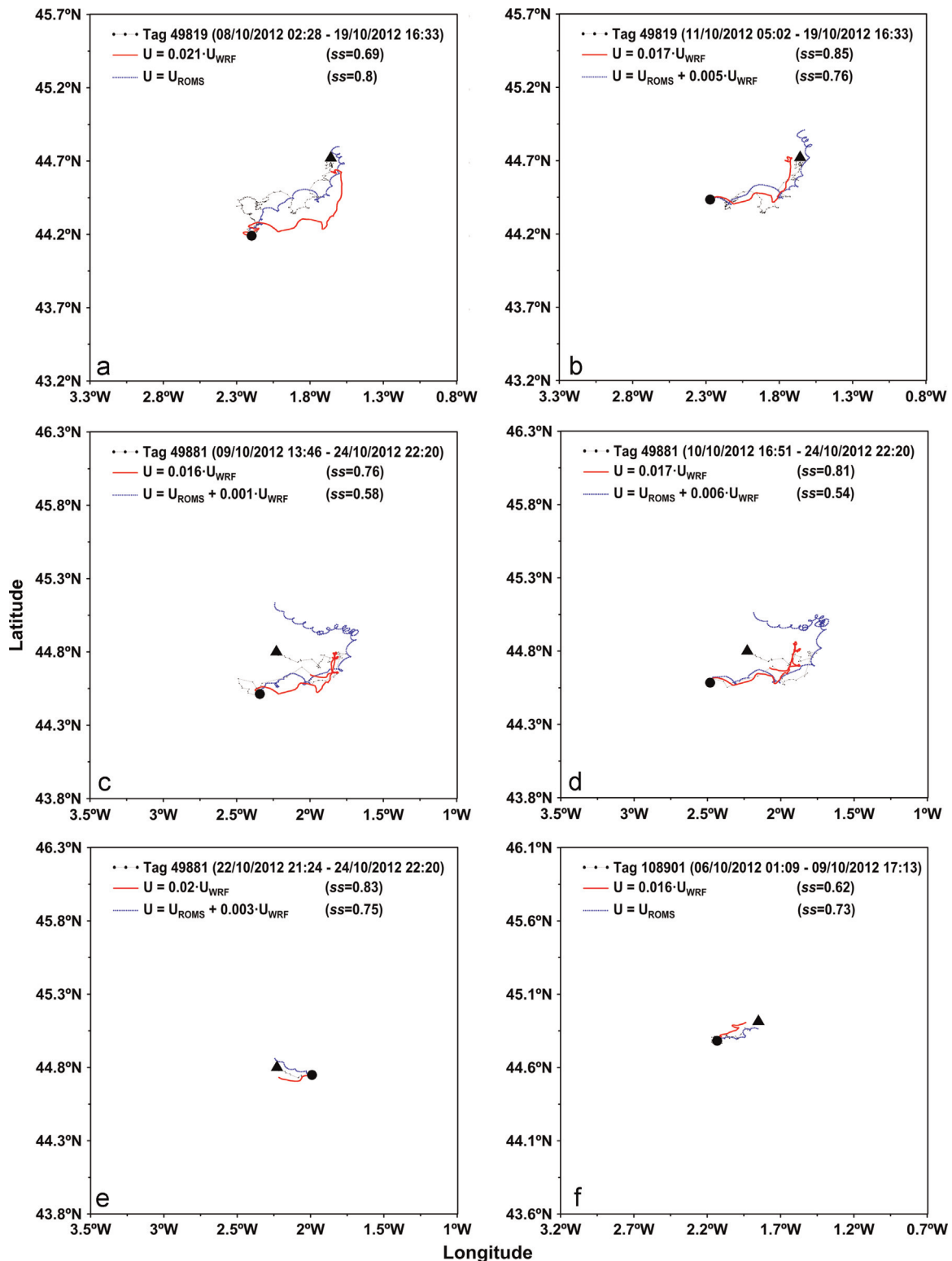


Fig. 7. Modeled and observed trajectories for the following tags and start dates: (a) 49819, 08/10/2012; (b) 49819, 11/10/2012; (c) 49881, 09/10/2012; (d) 49881, 10/10/2012; (e) 49881, 22/10/2012; and (f) 108901, 06/10/2012. The symbols • and ▲ denote the tag locations on the start and end dates, respectively.

by currents, sending their locations. Therefore, their trajectories during this period can be used for model calibration. To our knowledge, it is the first time these tags are used for this purpose in the Bay of Biscay.

In the operational system, two types of forecasts are performed with SOFT: (1) Using virtual sightings of Portuguese man-of-war.

Every day, particles are released at 52 fixed points located between the coast and 43.7°N in latitude, and between 3.4°W and 1.6°W in longitude (Fig. 6a). These particles are dispersed for 96 h, starting at 00:00 GMT; and (2) using real sightings of Portuguese man-of-war. This simulation is only run when SOS-Deiak provides to AZTI with information of real sightings. It is not necessary to run SOFT

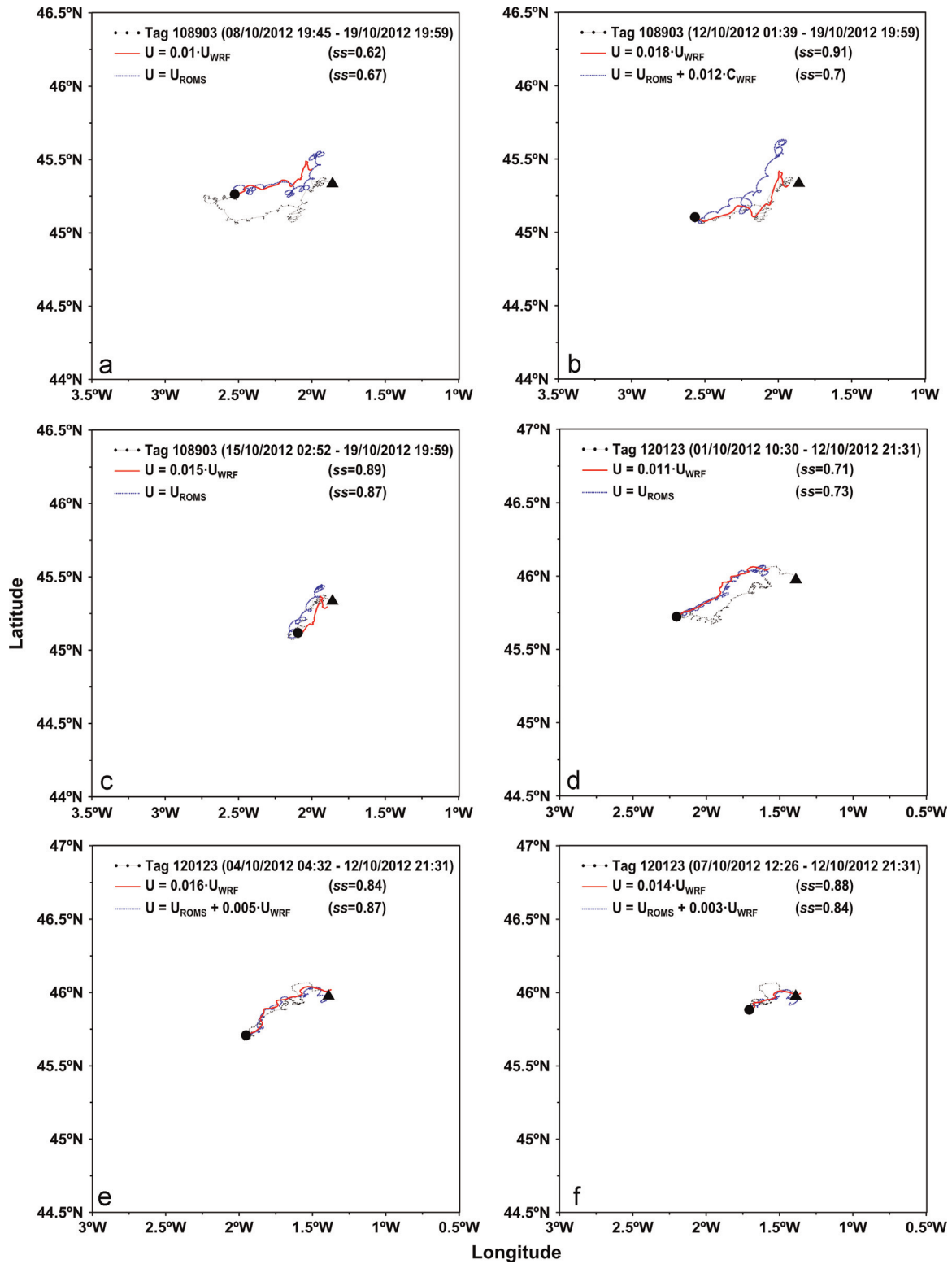


Fig. 8. Modeled and observed trajectories for the following tags and start dates: (a) 108903, 08/10/2012; (b) 108903, 12/10/2012; (c) 108903, 15/10/2012; (d) 120123, 01/10/2012; (e) 120123, 04/10/2012; and (f) 120123, 07/10/2012.

when the Portuguese man-of-war is observed within a bay or enclosed coastal area, or if it has already reached the coastline. When this happens, it could be of interest to estimate the region of origin of this Portuguese man-of-war. This is possible by means of a backward in time simulation.

3. Results

In 2012, there were a total of 41 sightings of Portuguese man-of-war along the Basque Country coast, nine of which occurred in August at Zarautz beach (Table 1). August was the month with the

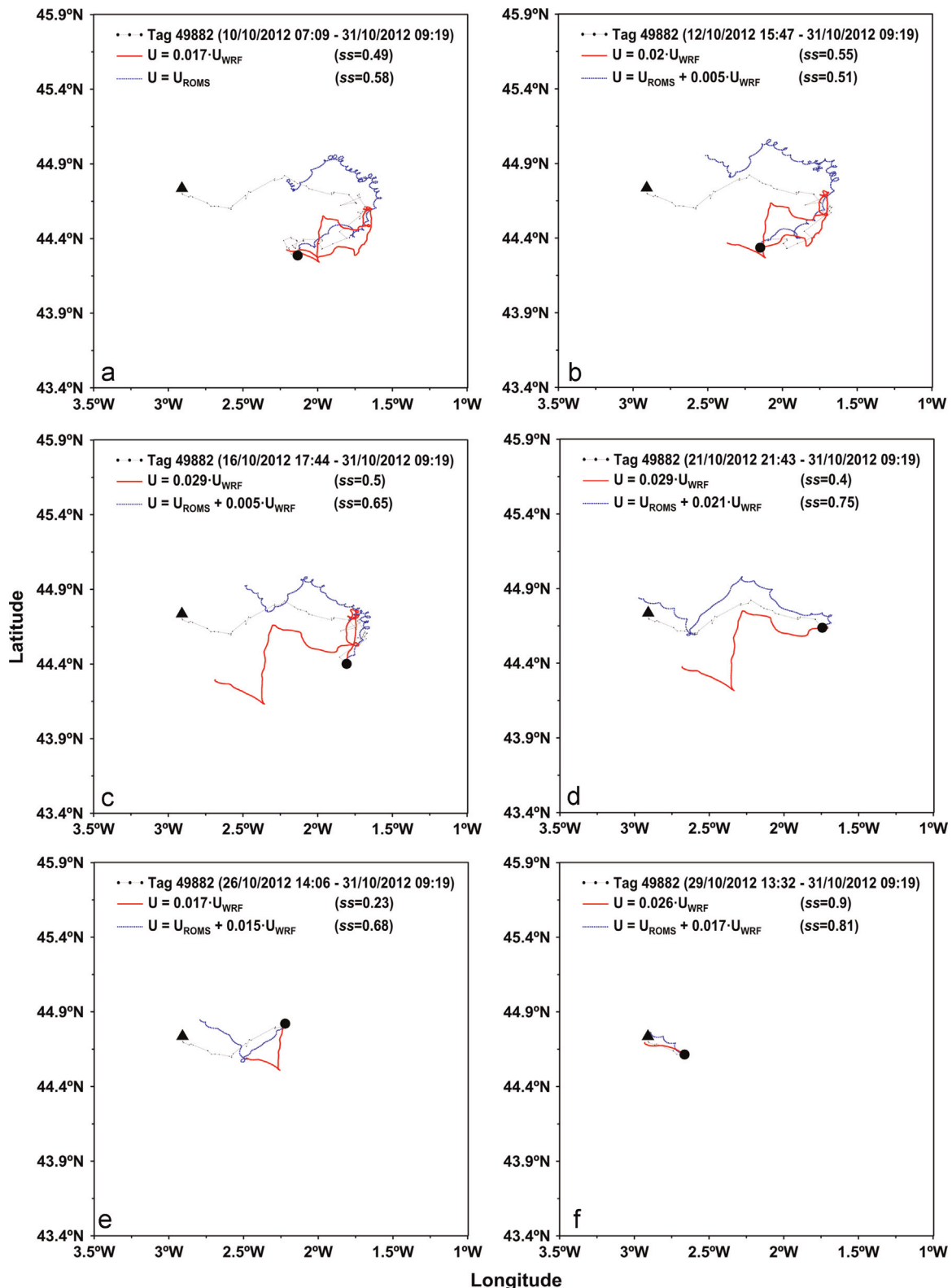


Fig. 9. Modeled and observed trajectories for tag 49882, starting on the following dates: (a) 10/10/2012; (b) 12/10/2012; (c) 16/10/2012; (d) 21/10/2012; (e) 26/10/2012; and (f) 29/10/2012.

highest number of sightings, with a total of 31, while in July and September only eight and two sightings were registered, respectively. In 2013, this number decreased to a total of seven: four in July and three in May, June and August. Fig. 6b shows the number of sightings grouped by coastal areas. In the Zarautz beach area, there were a total of 21 sightings.

In contrast to 2010, the years 2012 and 2013 can be considered as relatively calm since few sightings of Portuguese man-of-war were registered along the Basque Country coast. In the summer of 2010, the security operation adopted by the Department of Beaches of the City Council of Donostia-San Sebastián picked up more than 3,500 Portuguese man-of-war. The summer of 2012 was the

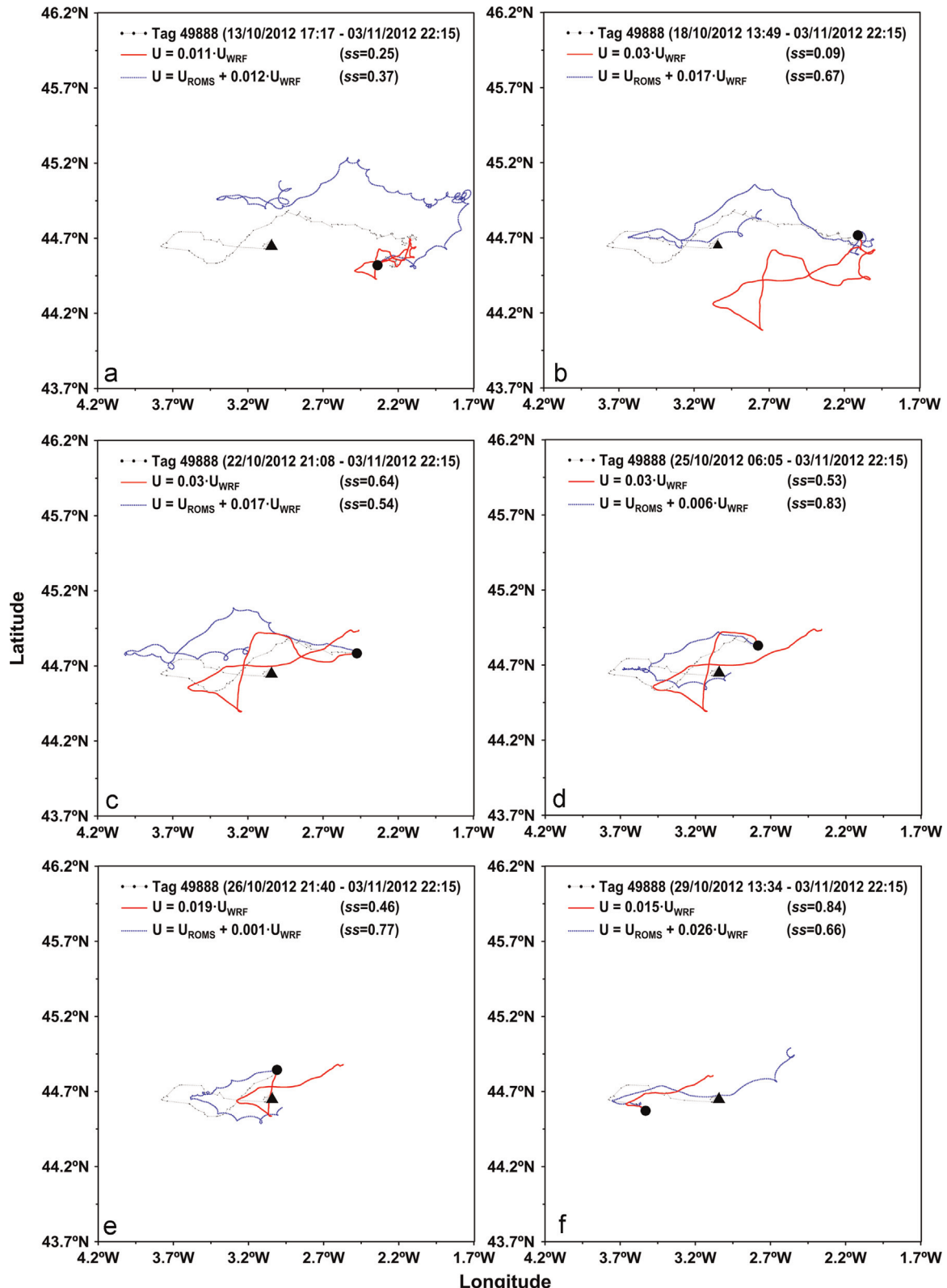


Fig. 10. Modeled and observed trajectories for tag 49888, starting on the following dates: (a) 13/10/2012; (b) 18/10/2012; (c) 22/10/2012; (d) 25/10/2012; (e) 26/10/2012; and (f) 29/10/2012.

first time in which both daily simulations with virtual sightings and specific simulations with several real sightings were carried out with SOFT, resulting in forecast reports for SOS-Deiak.

As mentioned above, trajectories from satellite pop-up tags for fish tracking were used for the modeling system calibration.

Figs. 7–11 show the modeled and observed trajectories for eight tags: 49819, 49881, 49882, 49888, 49889, 108901, 108903 and 120123. These tags were sending GPS locations during the battery lifetime (between three days and three weeks), in October–November 2012 (Table 2). All the received GPS locations with an

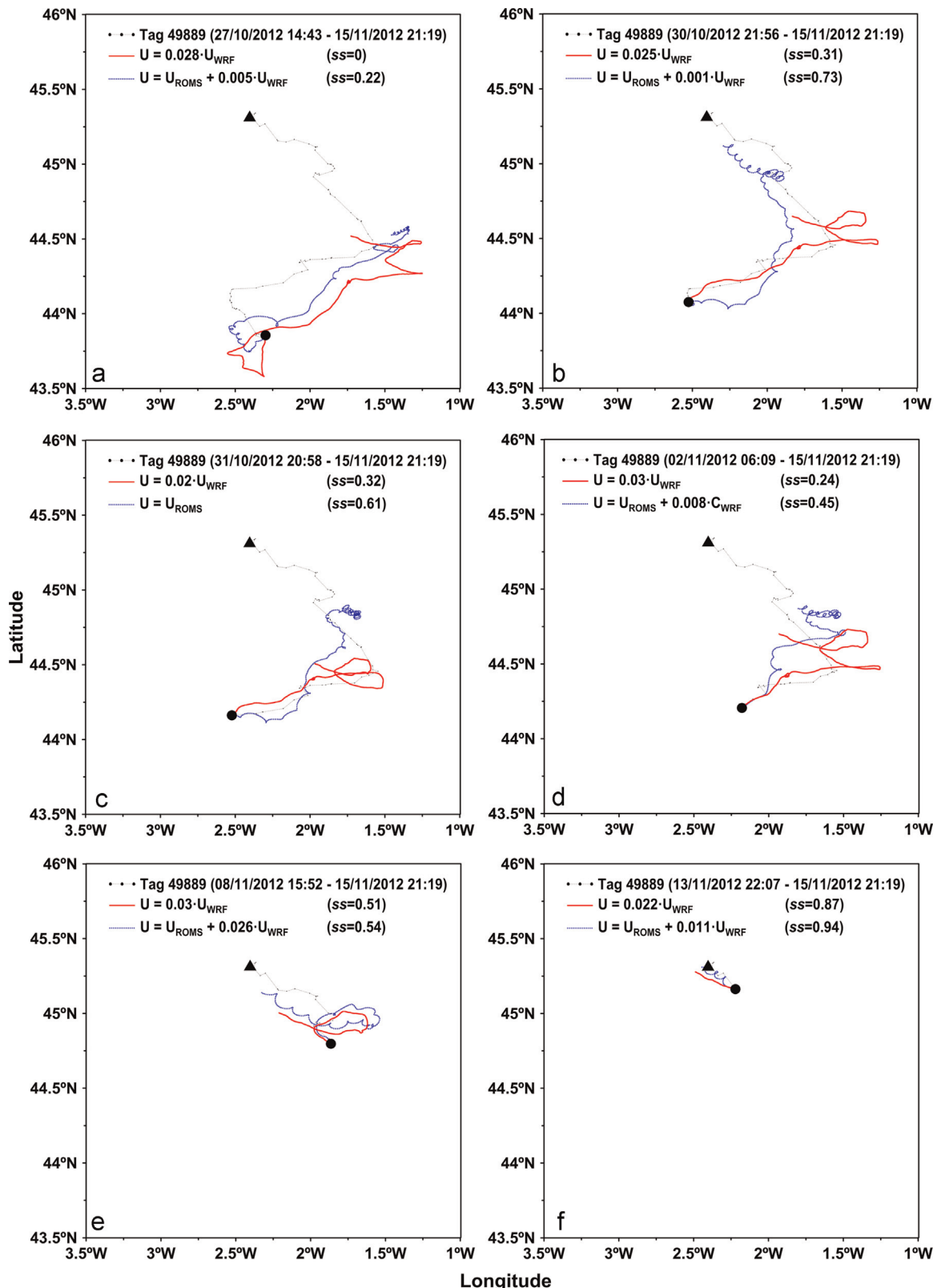


Fig. 11. Modeled and observed trajectories for tag 49889, starting on the following dates: (a) 27/10/2012; (b) 30/10/2012; (c) 31/10/2012; (d) 02/11/2012; (e) 08/11/2012; and (f) 13/11/2012.

estimated error lower than 1.5 km are shown in Figs. 7–11. In these figures, the trajectories simulated with SOFT are those with the optimal C_{ROMS} and C_{WRF} values (i.e., with the lowest s value among all the simulations carried out for each tag). On the one hand, two types of simulations were performed with SOFT to

simulate the tag trajectories and obtain the optimal C_{ROMS} and C_{WRF} values: (1) Using only the WRF wind velocities in SOFT to estimate the tag drift ($C_{ROMS}=0$ and $C_{WRF}=[0,0.04]$); and (2) using the ROMS current velocities with or without the WRF wind velocities ($C_{ROMS}=1$ and $C_{WRF}=[0,0.04]$) to estimate this drift. On the

Table 2

Start and end dates of the tag trajectories observed in October–November 2012 in the Bay of Biscay.

Tag	Start date (dd/mm/yyyy hh:mm)	End date (dd/mm/yyyy hh:mm)
49819	08/10/2012 02:28	19/10/2012 16:33
49881	09/10/2012 13:46	24/10/2012 22:20
49882	10/10/2012 07:09	31/10/2012 09:19
49888	13/10/2012 17:17	03/11/2012 22:15
49889	27/10/2012 14:43	15/11/2012 21:19
108901	06/10/2012 01:09	09/10/2012 17:13
108903	08/10/2012 19:45	19/10/2012 19:59
120123	01/10/2012 10:30	12/10/2012 21:31

other hand, several trajectories were estimated with SOFT for each tag. The first of these trajectories covers the whole period of the observed tag trajectory, while the remaining ones start on different dates and from different GPS locations. Only those GPS locations with an estimated error lower than 250 m were used as initial points for the modeled trajectories. Following this methodology, it is possible to verify whether the modeling system is able to simulate the whole observed tag trajectory or only part of it.

The sea surface drift depends on the characteristics of the object being moved (weight, density, shape, etc.). The tags used for the modeling system calibration have a length of approximately 31 cm (including the antenna), a maximum diameter of 3.2 cm and a weight of 40 g (Fig. 5). On average, the Portuguese man-of-war that reach the Basque Country coast are small and have a weight and density similar to these tags, but the shape is different. Therefore, it is expected that the tag drift is similar to the movement of particles in the upper water layer (i.e., highly complex). In this sense, the accuracy of the wind and current fields used in SOFT is crucial to obtain a robust result.

Figs. 7 and 8 show the modeled and observed trajectories for tags 49819, 49881, 108901, 108903 and 120123. When using only the WRF wind velocities in SOFT, the optimal C_{WRF} value for those modeled trajectories with $ss > 0.8$ ranges from 0.014 to 0.02. In general, the WRF wind velocities are not able to simulate the whole observed trajectories (i.e., $ss \leq 0.8$). However, some parts of these trajectories are satisfactorily resolved with the WRF wind velocities (see Figs. 7b, d, e, 8b, c, e and f, with $ss > 0.8$). When using the ROMS current velocities in SOFT (with or without the WRF wind velocities), the results are worse or similar. In this case, the trajectories shown in Fig. 8c, e and f have a C_{WRF} value of 0, 0.005 and 0.003, respectively.

Figs. 9, 10 and 11 show the modeled and observed trajectories for tags 49882, 49888 and 49889, respectively. For these tags, the trajectories are highly complex and none of the velocity inputs used in SOFT is able to adequately reproduce the whole observed trajectories. When using only the WRF wind velocities in SOFT, the optimal C_{WRF} value for those modeled trajectories with $ss > 0.8$ is 0.026 (Fig. 9f), 0.015 (Fig. 10f) and 0.022 (Fig. 11f). When using the ROMS current velocities in SOFT (with or without the WRF wind velocities), the results are similar for tags 49882 and 49889, with a C_{WRF} value of 0.017 and 0.011, respectively (Figs. 9f and 11f). For tag 49888, the best modeled trajectory is shown in Fig. 10d, with a C_{WRF} value of 0.006. Although some parts of the observed trajectories are simulated with the WRF wind and ROMS current velocities, it seems clear that the possible spatio-temporal deviations between the modeled and observed wind fields and their higher variability (in module and direction) lead to worse results than for the tags shown in Figs. 7 and 8. Unfortunately, these deviations cannot be proved because, in general, there are no hourly wind observations in the area where a tag is moving.

The results obtained for tags 49819, 49881, 108901, 108903 and

120123 (Figs. 7 and 8) suggest that under conditions of low or gradual variability in wind direction the WRF wind velocities could be applied to estimate the tag drift. This is especially true with winds from the southern and western sectors (third quadrant). On the contrary, the results obtained for tags 49882, 49888 and 49889 (Figs. 9–11) suggest that, in general, the surface drift of these objects is highly complex and largely dependent on the accuracy of the WRF wind fields used in the modeling system. In this case, the SOFT simulations carried out with the ROMS current velocities do not improve the results, except for the trajectory shown in Fig. 10d. In summary, for those simulated trajectories with $ss > 0.8$, SOFT is able to reproduce the tag drift using surface current velocities estimated as ~ 0.018 of the WRF wind velocities (lower than the 0.03 value applied in the drift of oil spills).

Finally, Fig. 12 shows the SOFT results obtained with a 148-d backward in time simulation that starts on 28 May 2013 (at 18:18 local time) and uses a real sighting of Portuguese man-of-war (found at La Zurriola beach). In this case, SOFT used only the WRF wind velocities with two different C_{WRF} values: (a) 0.013; and (b) 0.02. SOFT was run backward in time in order to estimate the location of this organism on 1 January 2013, which is the end date of the simulation. The results show that the use of a lower C_{WRF} value decreases the distance traveled by the Portuguese man-of-war in the 148-d backward in time simulation, implying that its location on 1 January 2013 is closer to the Cantabrian coast. Therefore, C_{WRF} is a crucial parameter to estimate the drift of Portuguese man-of-war, especially under strong wind conditions. This parameter could be adjusted with higher accuracy through the analysis of data from Portuguese man-of-war shaped drifting buoys.

4. Discussion

This work summarizes our effort to estimate the drift of Portuguese man-of-war using outputs from numerical models. In general, ocean circulation models, such as the ROMS version used in this study, resolve the standard Ekman currents, tides, and inertial currents, but do not include the effects of wind and waves in the upper centimeters of the water column. This is a valid approximation for those studies in which the aforementioned effects are not the central interest. In our case, these effects can be significant and must be taken into account, as shown several papers. The results of some of these papers are summarized below.

Perrie et al. (2003) used a three-dimensional diagnostic model together with an operational wave forecasting model to analyze the effects of wind and waves. They found that the wave-modified current can exceed the standard Ekman current by as much as 40% in rapidly developing intense storms. A large part of this increase in current velocity can be attributed to the Stokes drift. Dunlap et al. (2004) compared drifter trajectories with results obtained using the Princeton Ocean Model (POM) with and without the sea wave-induced Stokes drift correction ($\sim 2\text{--}2.5\%$ of the wind velocity). These authors also used an empirical wind model, where the surface current velocity was estimated as 3.3% of the wind speed with 20° to the right of the wind direction. In their work, they used 48-h forecasts of 30-m averaged currents from POM (every two hours) and winds from the Canadian Meteorological Center (at six hourly synoptic times). They concluded that the POM surface currents with the Stokes drift improved significantly the predictions in comparison with those obtained without the Stokes drift and from the empirical wind model.

Tang et al. (2007) also investigated the effects of waves on surface currents using a coupled wave–ocean–drifter model, based on Jenkins' formulation and velocity data derived from surface drifters. In their model, the total surface current was the sum of

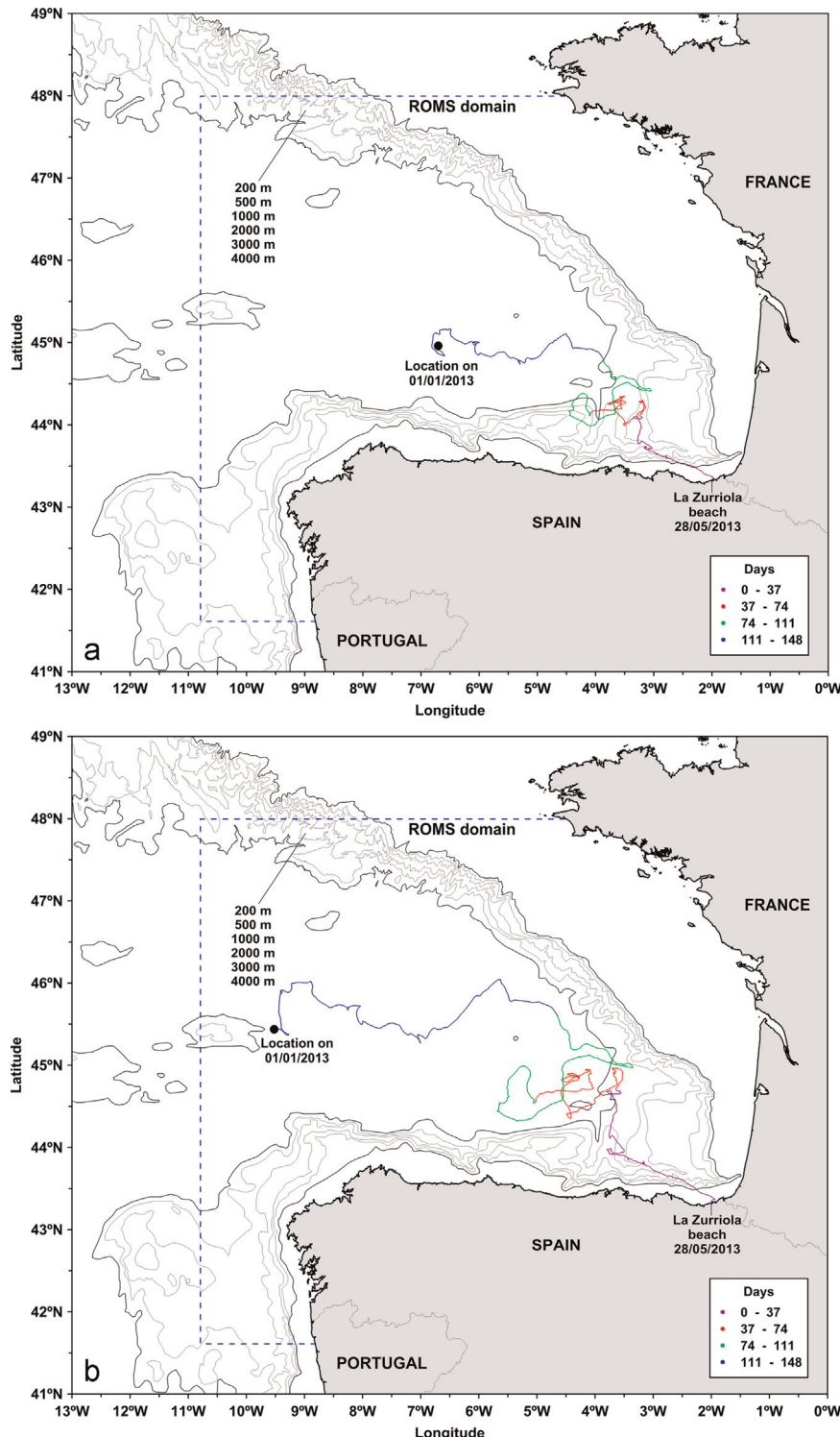


Fig. 12. SOFT results obtained with a 148-d backward in time simulation that starts on 28 May 2013 (at 18:18 local time) and uses a real sighting of Portuguese man-of-war. The drift of this Portuguese man-of-war (found at La Zurriola beach) and its location on 1 January 2013 were estimated using only the WRF wind velocities in SOFT with two different C_{WRF} values: (a) 0.013; and (b) 0.02.

the wave-modified current, the Stokes drift (estimated from the wave energy spectrum), and the tidal current. There are two major wave effects in Jenkins' theory: the Stokes drift and the air–wave-current momentum transfers. In their results, the Stokes drift was the dominant wave effect, increasing the surface drift speed by 35% and veering the current toward the wind direction. A statistical analysis of the modeled currents and drifter data showed that the inclusion of wave effects improved the model simulations

significantly. The modeled surface currents showed to be sensitive to the surface eddy viscosity and the wave energy spectrum.

Abascal et al. (2009) calibrated a Lagrangian transport model using 13 buoys deployed in the Bay of Biscay during the Prestige accident together with meteorological and oceanographic outputs from numerical models. In their Lagrangian transport model, the total surface current was estimated using three components: the ocean current from the NLPOM and MERCATOR models, the wind

and sea wave-induced current calculated using the wind outputs from the HIRLAM model, and the swell wave-induced current obtained using the outputs from the WAM model. Three coefficients were used to calibrate these currents. They concluded that the buoys located outside the continental slope were mainly driven by the wind, whereas the ocean current played an important role in the movement of those buoys located over the continental slope and shelf. For the buoys located outside the continental slope, the wind drag coefficient ranged from 0.018 to 0.038.

In another paper, Abascal et al. (2012) demonstrated that HF radar currents combined with modeled winds are of value for the backtracking of floating objects. Their results suggest that under calm wind conditions HF radar currents could be used as a unique forcing to simulate the trajectories of surface drifting buoys with a small drogue (~60 cm). However, both HF radar currents and wind fields are required to simulate the trajectories of those buoys without a drogue. They found that, on average, 1.5% of the wind velocity was the optimal empirical model to estimate the wind-induced current.

These remarkable findings and our results suggest that the fastest and most effective way to estimate the complex drift of floating objects could be a simple empirical model based on the local wind around the object being moved. In this model, the surface current velocity would be estimated as a percentage of the wind velocity. For surface drifters such as the tags analyzed here, this percentage is lower than the typical 3% value used in the drift of oil spills (Fallah and Stark, 1976; Wu, 1983). On average, 1.8% of the wind velocity is an optimal value that agrees with those obtained by Abascal et al. (2009, 2012) with surface drifting buoys. Our results also reveal the importance of errors in wind forecasts. These errors are propagated to the ocean and wave models that use these forecasts.

While we have come a long way, we have a lot further to go. It seems obvious that to correctly account for the effects of wind and waves on surface currents, a fully coupled wave–ocean model is needed. Another point to consider is the trajectory comparison methodology. In this sense, it would be interesting to separate the whole observed trajectory into shorter trajectories with similar wind characteristics (module and direction) or 2-d trajectories. Following this methodology, we could analyze under which wind conditions SOFT is able to reproduce the observed trajectory or whether the model can be used beyond 48 h. These issues will be dealt with in future investigations.

5. Summary and conclusions

In the summer of 2012, an operational protocol for the sighting and tracking of Portuguese man-of-war was established in the southeastern Bay of Biscay. This action protocol combines sightings of organisms at sea with their tracking through 96-h forecasts of their drift. These forecasts are performed with the Sediment, Oil spill and Fish Tracking model (SOFT), using hourly surface currents and winds obtained with the Regional Ocean Modeling System (ROMS) and the Weather Research and Forecasting model (WRF), respectively. In 2012 and 2013, there were a total of 48 sightings of Portuguese man-of-war along the Basque Country coast. Due to the lack of data about Portuguese man-of-war trajectories, the SOFT calibration was carried out using eight trajectories from satellite pop-up tags for fish tracking. These floating objects have a weight and density similar to the Portuguese man-of-war that reach the Basque Country coast. The SOFT calibration shows that the tag drift is a complex process, which is mainly controlled by the wind. This drift is largely dependent on the accuracy of the wind fields used in the modeling system. With winds from the southern and western sectors (third quadrant), SOFT is able to reproduce the tag drift using ~1.8% of the WRF wind velocities.

This percentage is lower than the 3% value applied in the drift of oil spills. The SOFT simulations performed using the ROMS current velocities (with or without the WRF wind velocities) do not improve the results. In the near future, improvements to numerically estimate the drift of these organisms at regional scale and to give more accurate information on their region of origin could include the following: (1) Outputs from higher resolution circulation models at global scale; and (2) trajectories from Portuguese man-of-war shaped drifting buoys. While the former would improve the inputs for the boundary conditions used in WRF and ROMS, the latter would provide data for the SOFT calibration.

Acknowledgments

The authors would like to thank Alicia Navarro, Casey Dunn, Eneko Fraile, Irati Epelde and Raúl Castro for their technical assistance, and the ROMS developers for their invaluable advice and comments at www.romsagrif.org. This research was supported by the Department of Education, Linguistic Policy and Culture of the Basque Government through the program “Proyectos de investigación básica y/o aplicada y proyectos en cooperación para el periodo 2013–2015”, within the PI2013-01 project. We would also like to thank the financial support received in the past from the Department of Industry, Innovation, Commerce and Tourism of the Basque Government (ETORTEK program, ITSASEUS project); the European Union (INTERREG IVa program, LOREA project); and the Spanish Ministry of Economy and Competitiveness (National Plan for Scientific and Technical Research and Innovation, CTM2013-45423-R project). This paper is contribution no. 694 from AZTI-Marine Research.

References

- Abascal, A.J., Castanedo, S., Fernández, V., Medina, R., 2012. Backtracking drifting objects using surface currents from high-frequency (HF) radar technology. *Ocean Dyn.* 62 (7), 1073–1089.
- Abascal, A.J., Castanedo, S., Mendez, F.J., Medina, R., Losada, I.J., 2009. Calibration of a Lagrangian transport model using drifting buoys deployed during the Prestige oil spill. *J. Coast. Res.* 25 (1), 80–90.
- Antonov, J.I., Seidov, D., Boyer, T.P., Locarnini, R.A., Mishonov, A.V., Garcia, H.E., Baranova, O.K., Zweng, M.M., Johnson, D.R., 2010. World Ocean Atlas 2009, Volume 2: Salinity. In: Levitus, S., (Ed.), NOAA Atlas NESDIS 69, U.S. Government Printing Office, Washington, D.C., 184pp.
- Bardi, J., Marques, A.C., 2007. Taxonomic redescription of the Portuguese man-of-war, *Physalia physalis* (Cnidaria, Hydrozoa, Siphonophorae, Cystonectae) from Brazil. *Iheringia Ser. Zool.* 97 (4), 425–433.
- Benson, D.J., 1992. Computational methods in Lagrangian and Eulerian hydrocodes. *Comput. Methods Appl. Mech. Eng.* 99 (2–3), 235–294.
- Caballero, A., Ferrer, L., Rubio, A., Charria, G., Taylor, B.H., Grima, N., 2014. Monitoring of a quasi-stationary eddy in the Bay of Biscay by means of satellite, in situ and model results. *Deep-Sea Res. Pt. II* 106, 23–37.
- Caballero, A., Espino, M., Sagarmina, Y., Ferrer, L., Uriarte, Ad., González, M., 2008. Simulating the migration of drifters deployed in the Bay of Biscay, during the Prestige crisis. *Mar. Pollut. Bull.* 56 (3), 475–482.
- Choi, B.-J., Wilkin, J.L., 2007. The effect of wind on the dispersal of the Hudson River plume. *J. Phys. Oceanogr.* 37 (7), 1878–1897.
- Condon, R.H., Duarte, C.M., Pitt, K.A., Robinson, K.L., Lucas, C.H., Sutherland, K.R., Mianzan, H.W., Boeberg, M., Purcell, J.E., Decker, M.B., Uye, S.-i., Madin, L.P., Brodeur, R.D., Haddock, S.H.D., Malej, A., Parry, G.D., Eriksen, E., Quiñones, J., Acha, M., Harvey, M., Arthur, J.M., Graham, W.M., 2013. Recurrent jellyfish blooms are a consequence of global oscillations. *Proc. Natl. Acad. Sci. U.S.A.* 110 (3), 1000–1005.
- Debreu, L., Marchesiello, P., Penven, P., Cambon, G., 2012. Two-way nesting in split-explicit ocean models: Algorithms, implementation and validation. *Ocean Model.* 49–50, 1–21.
- Di Lorenzo, E., Miller, A.J., Neilson, D.J., Cornuelle, B.D., Moisan, J.R., 2004. Modelling observed California current mesoscale eddies and the ecosystem response. *Int. J. Remote Sens.* 25 (7–8), 1307–1312.
- Dunlap, E., Tang, C.C.L., Wang, C.K., 2004. Comparison of model surface currents and drifter data from the Grand Banks. *Can. Tech. Rep. Hydrol. Ocean Sci.* 236 (vi+28pp).
- Egbert, G.D., Bennett, A.F., Foreman, M.G.G., 1994. TOPEX/POSEIDON tides estimated using a global inverse model. *J. Geophys. Res.* 99 (C12), 24821–24852.

- Ekman, V.W., 1905. On the influence of the Earth's rotation on ocean-currents. *Ark. Mat. Astron. Fys.* 2 (11), 1–52.
- Fairall, C.W., Bradley, E.F., Rogers, D.P., Edson, J.B., Young, G.S., 1996. Bulk parameterization of air-sea fluxes for tropical ocean-global atmosphere coupled-ocean atmosphere response experiment. *J. Geophys. Res.* 101 (C2), 3747–3764.
- Fairall, C.W., Bradley, E.F., Hare, J.E., Grachev, A.A., Edson, J.B., 2003. Bulk parameterization of air-sea fluxes: Updates and verification for the COARE algorithm. *J. Clim.* 16 (4), 571–591.
- Fallah, M.H., Stark, R.M., 1976. Random drift of an idealized oil patch. *Ocean Eng.* 3 (2), 83–97.
- Ferrer, L., Caballero, A., 2011. Eddies in the Bay of Biscay: A numerical approximation. *J. Mar. Syst.* 87 (2), 133–144.
- Ferrer, L., González, M., Cotano, U., Uriarte, A., Sagarminaga, Y., Santos, M., Uriarte, Ad., Collins, M.B., 2004. Physical controls on the evolution of anchovy in the Bay of Biscay: a numerical approximation. In: Proceedings of the ICES Annual Science Conference, 22–25 September 2004, Vigo, Spain, 20pp.
- Ferrer, L., González, M., Valencia, V., Mader, J., Fontán, A., Uriarte, Ad., Caballero, A., 2007. Operational coastal systems in the Basque Country region: modelling and observations. In: Chung, J.S., Kashivagi, M., Losada, I.J., Chien L.-K., (Eds.), Proceedings of the 17th International Offshore (Ocean) and Polar Engineering Conference, vol. 3, 1–7 July 2007, Lisbon, Portugal, pp. 1736–1743.
- Ferrer, L., Fontán, A., Mader, J., Chust, G., González, M., Valencia, V., Uriarte, Ad., Collins, M.B., 2009. Low-salinity plumes in the oceanic region of the Basque Country. *Cont. Shelf Res.* 29 (8), 970–984.
- Ferrer, L., Zaldúa-Mendizábal, N., Del Campo, A., Franco, J., Mader, J., Cotano, U., Uriarte, Ad., Aranda, J.A., 2013. Protocolo operacional para el avistamiento y seguimiento del cnidario *Physalia physalis* (carabela portuguesa) en el sureste del golfo de Bizkaia. *Rev. Investig. Mar.* 20 (7), 88–102.
- Fontán, A., Mader, J., González, M., Uriarte, Ad., Gyssels, P., Collins, M.B., 2006. Marine hydrodynamics between San Sebastián and Hondarribia (Guipúzcoa, northern Spain): field measurements and numerical modelling. *Sci. Mar.* 70S1, 51–63 (June 2006, Barcelona, Spain).
- González, M., Uriarte, Ad., Fontán, A., Mader, J., Gyssels, P., 2004. Marine dynamics. In: Borja, A., Collins, M. (Eds.), Oceanography and Marine Environment of the Basque Country, vol. 70. Elsevier Oceanography Series, Amsterdam, The Netherlands, pp. 133–157.
- Haidvogel, D.B., Arango, H.G., Hedström, K., Beckmann, A., Malanotte-Rizzoli, P., Shchepetkin, A.F., 2000. Model evaluation experiments in the North Atlantic Basin: simulations in nonlinear terrain-following coordinates. *Dyn. Atmos. Oceans* 32 (3–4), 239–281.
- Hasselmann, K., 1970. Wave-driven inertial oscillations. *Geophys. Fluid Dyn.* 1 (3–4), 463–502.
- Huang, N.E., 1979. On surface drift currents in the ocean. *J. Fluid Mech.* 91 (1), 191–208.
- Ibáñez, M., 1979. Hydrological studies and surface currents in the coastal area of the Bay of Biscay. *Lurralde* 2, 37–75.
- Iosilevskii, G., Weihs, D., 2009. Hydrodynamics of sailing of the Portuguese man-of-war *Physalia physalis*. *J. R. Soc. Interface* 6, 613–626.
- Jenkins, A.D., 1989. The use of a wave prediction model for driving a near-surface current model. *Dt. Hydrogr. Z.* 42, 133–149.
- Koutsopoulos, C., Le Cann, B., 1996. Physical processes and hydrological structures related to the Bay of Biscay anchovy. *Sci. Mar.* 60 (Suppl. 2), S9–S19.
- Laiz, I., Ferrer, L., Plomaritis, T.A., Charria, G., 2014. Effect of river runoff on sea level from in-situ measurements and numerical models in the Bay of Biscay. *Deep-Sea Res. Pt. II* 106, 49–67.
- Liu, Y., Weisberg, R.H., 2011. Evaluation of trajectory modeling in different dynamic regions using normalized cumulative Lagrangian separation. *J. Geophys. Res.* 116, C09013. <http://dx.doi.org/10.1029/2010JC006837> (13pp.).
- Locarnini, R.A., Mishonov, A.V., Antonov, J.I., Boyer, T.P., Garcia, H.E., Baranova, O.K., Zweng, M.M., Johnson, D.R., 2010. World Ocean Atlas 2009, Volume 1: Temperature. In: Levitus, S., (Ed), NOAA Atlas NESDIS 68, U.S. Government Printing Office, Washington, D.C., 184pp.
- Longuet-Higgins, M.S., 1953. Mass transport in water waves. *Phil. Trans. R. Soc. Lond. A* 245, 535–581.
- Longuet-Higgins, M.S., 1960. Mass transport in the boundary layer at a free oscillating surface. *J. Fluid Mech.* 8 (2), 293–306.
- Marchesiello, P., McWilliams, J.C., Shchepetkin, A., 2001. Open boundary conditions for long-term integration of regional oceanic models. *Ocean Model.* 3 (1–2), 1–20.
- Marchesiello, P., McWilliams, J.C., Shchepetkin, A., 2003. Equilibrium structure and dynamics of the California Current system. *J. Phys. Oceanogr.* 33 (4), 753–783.
- Penven, P., Lutjeharms, J.R.E., Marchesiello, P., Roy, C., Weeks, S.J., 2001. Generation of cyclonic eddies by the Agulhas Current in the lee of the Agulhas Bank. *Geophys. Res. Lett.* 28 (6), 1055–1058.
- Perrie, W., Tang, C.L., Hu, Y., DeTracey, B.M., 2003. The impact of waves on surface currents. *J. Phys. Oceanogr.* 33 (10), 2126–2140.
- Pingree, R.D., Le Cann, B., 1992a. Three anticyclonic Slope Water Oceanic eDDIES (SWODDIES) in the southern Bay of Biscay in 1990. *Deep-Sea Res. Pt. A* 39 (7–8), 1147–1175.
- Pingree, R.D., Le Cann, B., 1992b. Anticyclonic eddy X91 in the southern Bay of Biscay, May 1991 to February 1992. *J. Geophys. Res.* 97 (C9), 14353–14367.
- Pollard, R.T., 1970. Surface waves with rotation: An exact solution. *J. Geophys. Res.* 75 (30), 5895–5898.
- Puillat, I., Lazure, P., Jégou, A.M., Lampert, L., Miller, P.I., 2004. Hydrographical variability on the French continental shelf in the Bay of Biscay, during the 1990s. *Cont. Shelf Res.* 24 (10), 1143–1163.
- Serpette, A., Le Cann, B., Colas, F., 2006. Lagrangian circulation of the North Atlantic Central Water over the abyssal plain and continental slopes of the Bay of Biscay: description of selected mesoscale features. *Sci. Mar.* 70S1, 27–42 (June 2006, Barcelona, Spain).
- Shchepetkin, A.F., McWilliams, J.C., 2005. The regional oceanic modeling system (ROMS): a split-explicit, free-surface, topography-following-coordinate oceanic model. *Ocean Model.* 9 (4), 347–404.
- Skamarock, W.C., Klemp, J.B., Dudhia, J., Gill, D.O., Barker, D.M., Wang, W., Powers, J.G., 2005. A description of the Advanced Research WRF Version 2. NCAR Technical Note, NCAR/TN-468+STR, 88pp.
- Song, J.-B., 2009. The effects of random surface waves on the steady Ekman current solutions. *Deep-Sea Res. Pt. I* 56 (5), 659–671.
- Song, Y.T., Haidvogel, D.B., 1994. A semi-implicit ocean circulation model using a generalized topography-following coordinate system. *J. Comp. Phys.* 115 (1), 228–244.
- Sotillo, M.G., Álvarez Fanjul, E., Castanedo, S., Abascal, A.J., Menéndez, J., Emelianov, M., Olivella, R., García-Ladona, E., Ruiz-Villareal, M., Conde, J., Gómez, M., Conde, P., Gutiérrez, A.D., Medina, R., 2008. Towards an operational system for oil-spill forecast over Spanish waters: Initial developments and implementation test. *Mar. Pollut. Bull.* 56 (4), 686–703.
- Tang, C.L., Perrie, W., Jenkins, A.D., DeTracey, B.M., Hu, Y., Toulany, B., Smith, P.C., 2007. Observation and modeling of surface currents on the Grand Banks: A study of the wave effects on surface currents. *J. Geophys. Res.* 112, C10025. <http://dx.doi.org/10.1029/2006JC004028>.
- Totton, A.K., Mackie, G.O., 1960. Studies on *Physalia physalis* (L.). Part I. Natural History and Morphology. Part II. Behaviour and Histology. Discovery Reports. Cambridge University Press, Cambridge, UK, 30, 301–408.
- Ursell, F., 1950. On the theoretical form of ocean swell on a rotating earth. *Mon. Not. R. Astron. Soc. (Geophys. Suppl.)* 6, S1–S8.
- Wu, J., 1983. Sea-surface drift currents induced by wind and waves. *J. Phys. Oceanogr.* 13 (8), 1441–1451.